

# Multiple recycled aggregate properties analysed by X-ray microtomography

© 2018. This manuscript version is made available under the CC-BY-NC-ND 4.0 license <http://creativecommons.org/licenses/by-nc-nd/4.0/>

C. Thomas<sup>a,\*</sup>

[carlos.thomas@unican.es](mailto:carlos.thomas@unican.es)

J. de Brito<sup>b</sup>

V. Gil<sup>b</sup>

J.A. Sainz-Aja<sup>a</sup>

A. Cimentada<sup>a</sup>

<sup>a</sup>LADICIM (Laboratory of Materials Science and Engineering), University of Cantabria, E.T.S. de Ingenieros de Caminos, Canales y Puertos, Av./Los Castros 44, 39005 Santander, Spain

<sup>b</sup>CERIS-ICIST, Instituto Superior Técnico, Universidade de Lisboa, Av. Rovisco Pais, 1049-001 Lisbon, Portugal

\*Corresponding author.

---

## Abstract

This paper presents a novel technique used to analyse the volume of adhered mortar to the recycled aggregate. A computerized microtomograph ( $\mu$ CT) device was used to evaluate the volume of the aggregate, the volume of natural aggregate and the volume of adhered mortar. To this end, a natural aggregate has been characterized, using the  $\mu$ CT, with which a source concrete has been produced. Subsequently, the source concrete has been crushed to obtain a first cycle recycled aggregate. After the characterization of the first-generation of recycled aggregate, a new source concrete has been made with it to be subsequently crushed again obtaining a second-generation recycled aggregates. In the same way a third-generation recycled aggregate has been obtained and has been equally characterized. The results show that the compaction capacity of the aggregate is reduced after successive recycling. It has been possible to quantify how much the closed porosity of the recycled aggregate decreases with the number of times it is recycled. The loss of natural aggregate and increase of the volume of adhered mortar have also been evaluated using this technique.

---

**Keywords:** Waste; Recycled aggregate; Recycled aggregate concrete; Multiple recycling; Adhered mortar;  $\mu$ CT analysis

## 1 Introduction

The increasing production of construction and demolition waste (C&DW) and the ever-greater consumption of natural resources is forcing society to search for alternatives in order to reduce both. Fortunately, many studies have analysed the possibility of producing recycled aggregates (RA) using old concrete from C&DW [1-6], precast industries [7-10] and industry wastes [11-13]. However, the use of RA against the use of natural aggregate (NA) for structural concrete on material performance, environmental benefits and financial viability of the studies conducted so far do not fully demonstrate the choice of production of recycled aggregate concrete (RAC) with a significant advantage [14].

RA influences the physical and mechanical properties of RAC. The direct influence of the quality of RA on the durability is analysed in [7,15] showing that RA coming from precast-structural concretes is one of the most adequate in order to produce RAC. In terms of durability, the incorporation of recycled aggregate was responsible for worse results but did not compromise their use in structural concrete [16,17]. The properties of the interfacial transition zone (ITZ) have a significant impact on the macro mechanical properties of concrete [18]. X-ray computed axial tomography (CT) provides cross-sectional views of materials, components, and assemblies for non-destructive evaluation [19]. It can be used to examine concrete [20] and the high-resolution X-ray micro-CT allows modelling the permeability of cementitious materials [21]. On the one hand, the irregular surface of the old adhered mortar of the RA contributes to the improvement of the physical bond between the old and new cement matrix [22]. On the other hand, the lower mechanical resistance due to the adhered mortar contributes to reduce the compressive strength [15] and significantly so in the case of dynamic rather than static loading [3,23-25] but no significant influence of the recycled aggregate content on the durability performance of concrete exposed to aggressive environments is detected after years [26].

This paper presents a novel technique used to analyse the volume of adhered mortar to the recycled aggregate. A computerized microtomograph ( $\mu$ CT) device was used to evaluate the volume of the aggregate, the volume of natural aggregate and the volume of adhered mortar. To this end, a natural aggregate has been characterized, using the  $\mu$ CT, with which a source concrete has been produced. Subsequently, the source concrete has been crushed to obtain a first cycle recycled aggregate. After the characterization of the first-generation of recycled aggregate, a new source concrete has been made with it to be subsequently crushed again obtaining a second-generation recycled aggregates. In the same way, a third-generation recycled aggregate has been obtained and characterized. The effectiveness of using X-ray microtomography to access recycled concrete pore size and spatial distribution requires small samples in order to increase the resolution, which is still a drawback to overcome [22]. In the present case, representative samples of the recycled aggregates have been obtained and analysed.

## 2 Experimental program

Four aggregates divided in three fractions were studied. A natural limestone aggregate (NA) was used to produce a source concrete (SC). The SC was crushed to obtain a first-generation recycled aggregate (RA1). A second-generation recycled aggregate (RA2) was obtained from crushing the first recycled aggregate concrete (RAC1), made with the first-generation of recycled aggregate. In the same way, a third-generation recycled aggregate (RA3) has been obtained crushing the second recycled aggregate concrete (RAC2). RAC1 and RAC2 were produced using 100% recycled aggregate from the previous recycling cycle. In all of the cases, the cement, aggregates grading and target concrete characteristics (strength, slump and durability) were the same: compressive strength class C30/37; slump class S3 ( $125 \pm 15$  mm); exposure class XC3, limestone sand and Portland CEM I 42.5. The mix proportions, compressive strength and slump are presented in Table 1. Cement with low content of additions was used to avoid effects due to the increasing volume of adhered mortar. NA, RA1, RA2 and RA3 were divided in three coarse aggregate fractions in order to obtain the physical and mechanical properties of each one: 4–5.6, 5.6–8 and 8–11.2 mm, using three different techniques: classic methods, computerized micro-tomography ( $\mu$ CT) and scan electron microscopy (SEM).

**Table 1** Mix proportions (by  $m^3$ ) and main properties of concrete.

Concrete	SC	RAC1	RAC2
Sand (0–2) (kg)	732	732	732
Coarse aggregate (4–8) (kg)	205	183	171
Coarse aggregate (8–16) (kg)	443	396	371
Coarse aggregate (16–22) (kg)	327	292	274
Cement (CEM I 42.5) (kg)	350	350	350
Water (kg)	194	194	194
Extra water (kg)	0	40	49
Effective w/c ratio	0.55	0.55	0.55
Apparent w/c ratio:	0.55	0.67	0.69
Slump (cm)	12.4	12.6	12.1
Compressive strength (MPa)	55.9	54.1	53.3

### 2.1 Properties of the aggregate by classic methods

The densities and porosities were determined by displacement of water by immersion of the saturated samples and evaluation of the saturated and dry weights of the samples. The methods used are described below. The water absorption capacity of the aggregates NA, RA1, RA2 and, RA3 was determined by evaluating the open pore volume saturated with water using vacuum. The relationship between the volume of accessible pores and sample volume, obtained by evaluating the difference between saturated and dry weights, provides the porosity of the material.

The real density (without pores) was determined by crushing each fraction of aggregate and concrete to powder smaller than  $100 \mu m$  using an automatic agate mill. The closed porosity was calculated by the difference between the relative volume and the real volume. The open porosity was calculated by the difference between the apparent volume and the relative volume.

24 h absorption of the aggregates was determined following standard EN 1097-6:2014. The determination of loose bulk density and voids was performed following standard EN 1097-3:2014. The Los Angeles wear test intends to measure the resistance to fragmentation of the aggregate through the loss of mass. The tests were carried out according to standard EN 1097:2014. All the tests following the EN 1097 standard were performed before obtaining the final mix proportions (Faury). For this reason, the commercial natural aggregate and the aggregate resulting from crushing the SC and RC, not the 4-5.6, 5.6-8 and 8-11.2 mm fractions, were considered.

## 2.2 Computerized micro tomography

In order to analyse the properties of the samples, a computerized micro-tomograph was used. The equipment can provide qualitative and quantitative information of the tested specimens.

The  $\mu$ CT analysis consists, first, of a scanning phase in which an X-ray beam impinges on the sample at the same time as it rotates, obtaining a set of X-ray images that the computer will compose. A Skyscan1172  $\mu$ CT, similar to the one used by [28] in order to analyse concrete, with 80 kV and 100  $\mu$ A X-ray source, was used. With these parameters the resolution Voxel Size is 27  $\mu$ m. In the reconstruction, the linear absorption of each material was correlated with a shade of grey between 0 [black] and 255 [white] using the same parameters for all the specimens.

The image quantitative analysis software provides the volume of the different components, because the voxel intensity is proportional to the density of the material [22]. In this case it is possible to evaluate the volume of aggregate, the volume of natural aggregate, the volume of adhered mortar and the closed porosity of the sample. Regarding the qualitative analysis, this technique allows analysing how pores and aggregate are distributed. For the identification of the aggregate and cement paste phases, previous analyses were made using only, on the one hand, cement paste and, on the other hand, natural aggregate used in the research.

Each fraction of aggregate was introduced in a cylindrical container of 40 mm diameter. A sample of 25 mm height has been compacted for 20 s using a vibration table. After that, the sample was introduced into the  $\mu$ CT with the container. Each analysis, with the indicated parameters lasts approximately 10 h.

The properties of the coarse aggregate, obtained by  $\mu$ CT, were obtained as follows. The compaction index is obtained by dividing the volume occupied by the aggregate by the total analysed volume. The volume of aggregate (solid fraction) is obtained by adding the volume of the natural aggregate, the adhered mortar and the porosity. The total volume corresponds to the volume of a cylinder inscribed in the volume occupied by the sample. Therefore, the compaction index quantifies the volume of voids between aggregates. Closed porosity in % vol. is obtained by dividing the closed porosity volume, bigger than 27  $\mu$ m, by the aggregate volume. The NA volume is obtained by dividing the volume of NA by the total analysed volume. The adhered mortar is the percentage of adhered mortar found in the analysed volume of aggregate. Finally, the mortar index is the result of dividing the volume of adhered mortar by the volume of natural aggregate.

## 2.3 Scan electron microscopy

A scanning electron microscope, Carl Zeiss model EVO MA15, for the microstructural and elemental chemical analysis, was used. It uses as a lanthanum hexaboride filament as the electron source and secondary and backscattered electrons detectors and an Oxford Instruments X-ray detector. This SEM can work in low vacuum allowing the observation of samples without conductors nor need of metallization.

The SEM is equipped with an Energy Dispersive X-ray spectroscopy detector (EDX). Using the EDX technique, it is possible to obtain the chemical composition of the analysed materials. In this case, in order to obtain the chemical composition by weight and atomic percentage, a sample of each aggregate was crushed to 100  $\mu$ m powder and analysed by EDX.

## 3 Results and discussion

In this section, the obtained results are shown and analysed.

### 3.1 Physical and mechanical properties by classic methods

Table 2 presents the main physical properties of aggregates (NA, RA1, RA2 and RA3) and the Faury distribution obtained using pycnometer and separated in three fractions. The Faury distribution is the same mix proportion ratio used to make the concrete, but in this case only with aggregates between 4 and 11.2 mm. These coarse fractions represent 19% by weight of the aggregate. The fraction 4-5.6 mm Faury proportion corresponds to 5.7 wt.%. The fraction 5.6-8 mm represents 6.3 wt.%. and the fraction 8-11.2 mm 6.8 wt.%.

**Table 2** Physical properties of the coarse aggregate obtained by classic methods.

Aggregate	Fraction [mm]	Relative density [g/cm <sup>3</sup> ]	Real density [g/cm <sup>3</sup> ]	Closed porosity [% vol.]
NA	Faury	2.630	2.744	0.099

	4-5.6	2.677	2.832	0.134
	5.6-8	2.657	2.701	0.038
	8-11.2	2.639	2.786	0.127
RA1	Faury	2.505	2.662	0.895
	4-5.6	2.562	2.695	0.759
	5.6-8	2.539	2.707	0.958
	8-11.2	2.496	2.668	0.981
RA2	Faury	2.463	2.558	0.542
	4-5.6	2.505	2.606	0.576
	5.6-8	2.489	2.591	0.582
	8-11.2	2.474	2.558	0.479
RA3	Faury	2.418	2.505	0.496
	4-5.6	2.489	2.604	0.656
	5.6-8	2.455	2.506	0.291
	8-11.2	2.392	2.492	0.570

In all the cases, the density of the aggregate decreases as the aggregate size increases. A larger density difference between the smaller aggregate (4-5.6 mm) and the larger aggregate (8-11.2 mm) as the number of recycling generations was observed. The density of the aggregate used in the different recycled concrete mixes (Faury method) decreases with the number of recycling cycles. The density of NA is around 2.63 g/cm<sup>3</sup> while RA1, RA2 and RA3 present a density 4%, 6% and 8% lower, respectively.

In relation to the water absorption, the results show an increase with the number of recycling cycles. The increase of water absorption, [Table 3](#), was noticeable after the first cycle (4.55% increase), up by 2.31% after the second cycle and again up by 1.69% after the third cycle. As the number of cycles of recycling increases the aggregates absorb more water because of the increase of adhered mortar in each cycle. This also occurs in the case of the loose bulk density, voids volume and Los Angeles coefficient.

**Table 3** Physical and mechanical properties of the coarse aggregate obtained by classic methods.

Aggregate	W <sub>24</sub> [%wt.]	Loose bulk density [kg/m <sup>3</sup> ]	Voids [%vol.]	Los Angeles [%wt.]
NA	1.09	1355.1	47.6	27.93
RA1	5.64	1132.2	55.2	38.81
RA2	7.95	1034.4	59.3	41.18
RA3	9.64	990.1	62.7	40.89

### 3.2 Computerized micro tomography

[Table 4](#) presents the main properties of aggregates (NA, RA1, RA2 and RA3) obtained by  $\mu$ CT. It is observed that the NA is the one that has a higher volume of aggregate. The aggregate here represents the coarse fraction and

the sand (<4 mm) has not been considered. The RA1 set presents a volume between aggregate 3% greater than that of the NA and this value increases slightly with the number of recycling cycles. If the compaction indexes of the various fractions are compared, the 4-5.6 mm fraction occupying higher volume is noticed and this value decreases with the number of recycling cycles.

**Table 4** Properties of the coarse aggregate obtained by  $\mu$ CT.

Aggregate	Fraction [mm]	Compaction index [% vol.]	Closed porosity [% vol.]	NA volume [% vol.]	Adhered mortar [% vol.]	Mortar index [% vol.]
NA	Faury	60.350	0.044	60.350	0.000	0.000
	4-5.6	60.877	0.030	60.877	0.000	0.000
	5.6-8	61.015	0.026	61.015	0.000	0.000
	8-11.2	60.978	0.073	60.978	0.000	0.000
RA1	Faury	57.605	0.713	25.355	55.489	1.268
	4-5.6	59.794	0.978	27.910	53.322	1.142
	5.6-8	59.413	0.667	26.318	55.704	1.258
	8-11.2	55.724	0.554	23.048	58.639	1.418
RA2	Faury	57.051	0.627	13.223	76.053	3.299
	4-5.6	57.270	0.632	14.458	74.755	2.961
	5.6-8	58.136	0.576	13.433	76.893	3.328
	8-11.2	57.459	0.686	12.367	78.476	3.646
RA3	Faury	56.586	0.524	6.310	87.885	8.203
	4-5.6	54.617	0.470	8.022	85.313	5.809
	5.6-8	57.279	0.471	6.074	89.395	8.430
	8-11.2	59.163	0.631	5.275	91.085	10.217

NA is, as expected, the least porous aggregate. The closed porosity of the recycled aggregate is 12 to 16 times higher than that of the NA. However, as the number of recycling cycles increases, the closed porosity (measured by  $\mu$ CT) decreases. The open porosity of RA increases with the number of recycling cycles by increasing the volume of adhered mortar. The porosity of cement paste at 1, 7 and 28 days found by [21] and analysed by microtomography was 27.3%, 18.9% and 13.5%, respectively. However, it is observed that the closed porosity decreases. The  $\mu$ CT technique only considers pores with a volume greater than  $0.08 \text{ mm}^3$  and does not consider the porosity communicating with the exterior through capillarity.

For the second and third generation of recycled aggregates, there is a trend of closed porosity to increase with the size of the aggregate and a greater concentration of porosity is observed in the attached mortar. Fig. 1 shows the volume of natural aggregate analysed in the upper row and the distribution of closed pores in the lower row. Fig. 2 shows the volume analysed and the porosity, in this case, of the RA1, Fig. 3 the RA2 and Fig. 4 the different fractions of RA3.

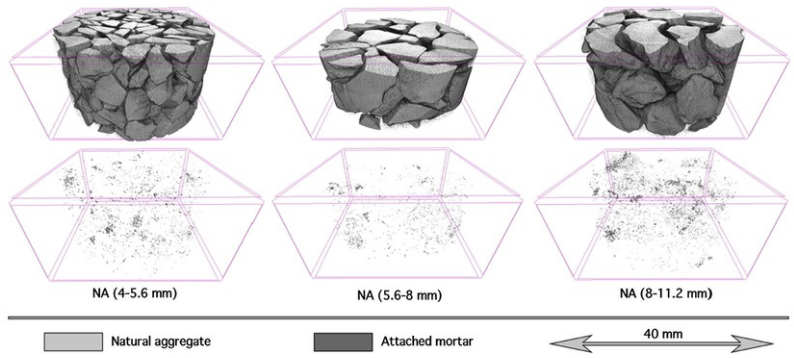


**Fig. 1** Analyzed volume (upper row) and closed porosity (lower row) of the different fractions of the coarse natural aggregate.

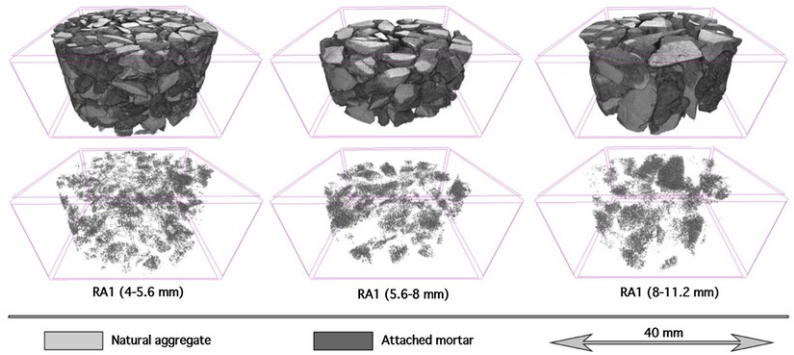


**Fig. 2** Analyzed volume (upper row) and closed porosity (lower row) of the different fractions of the first-generation recycled aggregate.

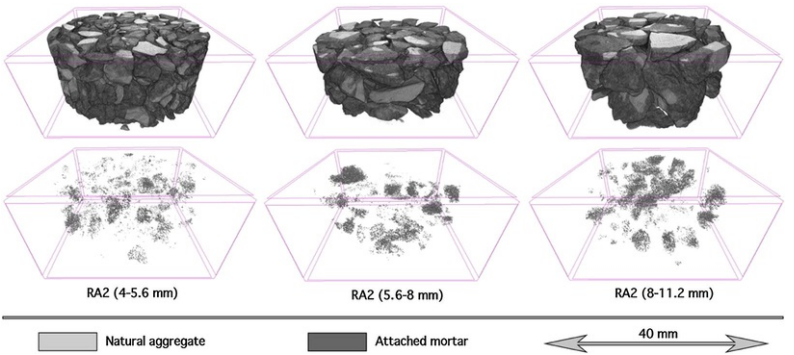


**Fig. 3** Analyzed volume (upper row) and closed porosity (lower row) of the different fractions of the second-generation recycled aggregate.

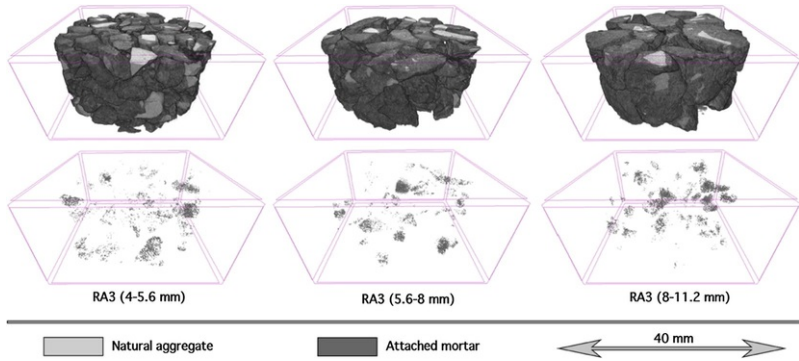


**Fig. 4** Analysed volume (upper row) and closed porosity (lower row) of the different fractions of the third-generation recycled aggregate.

The NA takes around 60% of the analysed volume. Sunayana and Barai [29] found 73% of occupied volume (maximum experimental packing density) using coarse and fine recycled aggregate. The decrease of the compaction index is due to the increase of porosity of the RA, at the same time that the volume of adhered mortar increases. The  $\mu$ CT consider the open porosity of the sample as non-occupied volume. The more rounded aggregate [22] tends to be better-packed (decrease of inter-aggregate voids) but the ratio between the volume of the solid fraction and the volume occupied by the aggregate decreases.

When the first generation of recycled aggregate is produced, the amount of natural aggregate present in RA1 is reduced by up to 25%. For this reason, 25% vol. of natural aggregate is expected in the first-generation recycled aggregate concrete (RAC1). The amount of natural aggregate present decreases to 13% and 6% with successive generations of recycling: RA2 and RA3. Due to this trend, with each generation of recycling, the natural aggregate/adhered mortar ratio decreases and a maximum number of cycles is expected until the presence of coarse natural aggregate is reduced to near zero values.

In Fig. 5, the natural aggregate/adhered mortar ratio has been represented versus the number of recycling cycles and a good exponential trend line has been obtained. It is thus found that the coarse natural aggregate becomes negligible between the fourth and the fifth cycle.

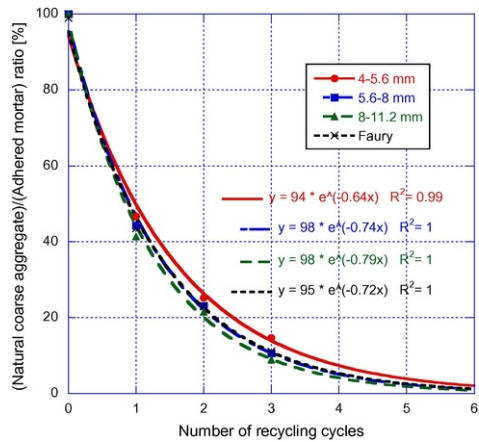


**Fig. 5** Natural coarse aggregate and adhered mortar volume ratio of the coarse recycled aggregate versus the number of recycling cycles.

Fig. 6 shows a section sequence of the NA, RA1, RA2 and RA3 fractions where the adhered mortar has been coloured green. The sequence confirms the trend obtained by the analytical methods. It can be observed how the green colour, corresponding to the adhered mortar in the successive recycling cycles, increases its presence. At the same time, it can be seen how the natural aggregate volume is reduced and its particles become smaller and smaller.



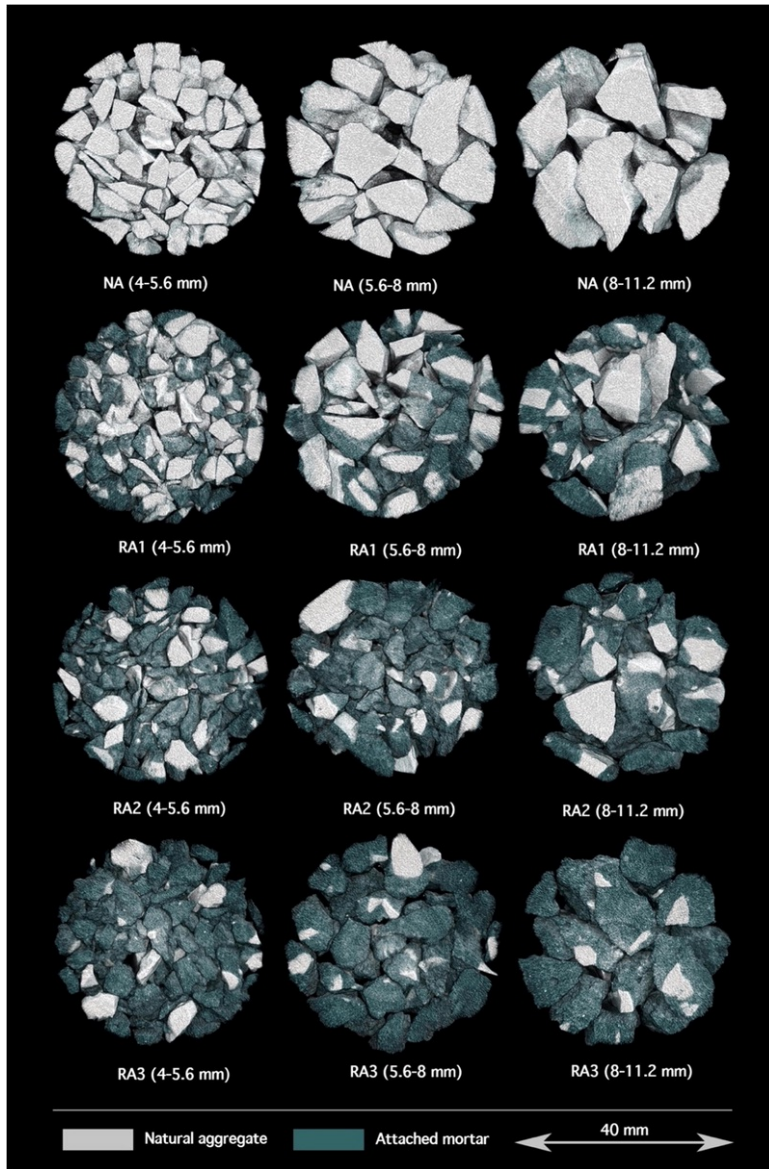


**Fig. 6** Analysed section of the natural and recycled coarse aggregate samples where the adhered mortar has been coloured green.

Several authors have attempted to measure the volume of adhered mortar to the natural aggregate of the recycled aggregate, by physical treatment [30] or chemical treatment [31]. It is well known that the decrease in the performance of the recycled aggregate is mainly due to the presence of this phase. The technique proposed here allowed easily evaluating the amount of adhered mortar.

In the mix distribution of the first generation recycled aggregate concrete, using RA1, 55% of the aggregate volume has been found to be adhered mortar. It is also observed that, with the increase of recycling cycles, the volume of adhered mortar increases to 76% for RA2 and 87% for RA3. In addition, a smaller amount of mortar is detected in the smaller fractions. The 4-5.6 mm first-generation recycled aggregate presents 5% less adhered mortar than the 8-11.2 mm fraction. Fig. 7 shows the adhered mortar volume for the different fractions versus the number of recycling cycles. A logarithmic trend line is obtained. It can be seen that the coarser fraction has an even higher



volume of adhered mortar than the finer one and the difference between them increase with the number of recycling cycles. Fraction 8-11.2 mm reaches 100% of mortar shortly after it exceeds the fourth recycling cycle, whereas the fraction 4-5.6 mm requires more than five recycling cycles to reach the same value of mortar. The mixture of the different fractions, in order to construct the skeleton of aggregates of concrete, is somewhere between the trend lines of the fractions analysed above and it reaches 100% of mortar only after between four and five recycling cycles.

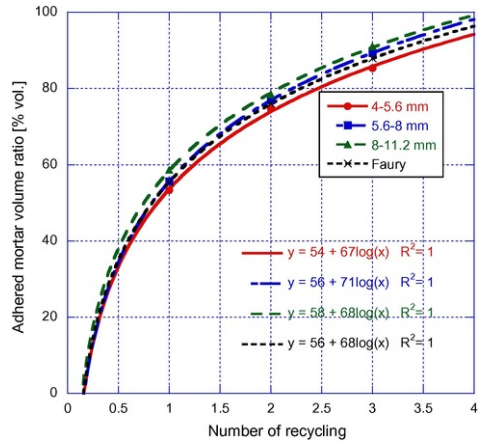


**Fig. 7** Adhered mortar volume of the coarse recycled aggregate versus the number of recycling cycles.

Comparing the absorption of the aggregate obtained by classic methods with the adhered mortar volume (Fig. 8), a linear correlation is obtained. The percentage of water that the aggregate is able to absorb is directly proportional to 10% of the volume of adhered mortar ( $W_{24} = 0.1V_{\text{AdheredMortar}}$ ). The relationship between the relative density of the aggregate and the volume of adhered mortar also presents a linear correlation. The density of the aggregate shows a strong decrease after the first recycling cycle, being the decrease smaller with the second and third cycles, in a similar way to what happens with the volume increase of adhered mortar.

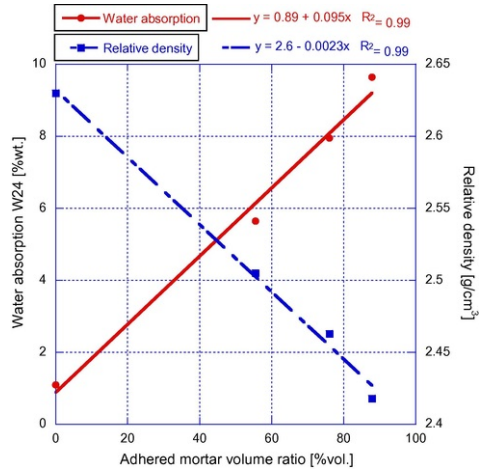


**Fig. 8** Water absorption and relative density versus adhered mortar volume of the coarse recycled aggregate.

Fig. 9 shows the correlation between the closed porosity obtained by the proposed  $\mu\text{CT}$  method and by classic methods. The linear adjustment between both values has an  $R^2$  of 0.72. Around the low closed porosity values, it is observed that all the results provided by the classic methods are lower than those provided by  $\mu\text{CT}$ . This effect may be due to the difficulty of saturating the accessible pores (classic method). In samples with low porosity, the classic method fails to saturate a given volume of open pores that will be evaluated, by the method, as closed pores. When the closed porosity of samples with higher porosity is examined, a greater dispersion is observed. However, the trend line places the values of closed porosity obtained by classic methods (water saturation) at around 80% of that obtained by  $\mu\text{CT}$ . The  $\mu\text{CT}$  technique demonstrates that there is a volume of open pores that cannot be accessed by classic

methods, especially when the porosity of the aggregate is low.

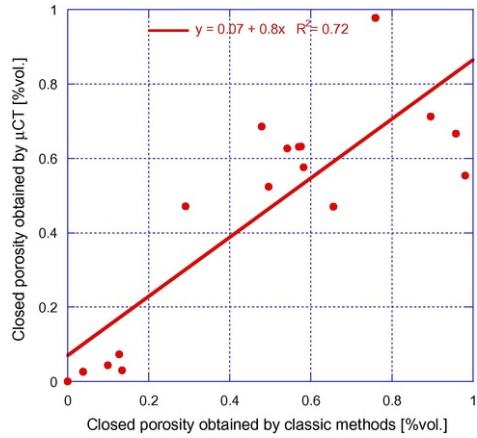


**Fig. 9** Closed porosity obtained the proposed method versus classic method.

### 3.3 Scan electron microscopy

Table 5 shows the elemental chemical composition of the control and recycled aggregates.

**Table 5** Elemental chemical composition of the recycled aggregates obtained by SEM.

Elem.	O		C		Si		Ca		Al		S		K		
	Quant.	Atm.%	wt.%	Atm.%	wt.%	Atm.%	wt.%	Atm.%	wt.%	Atm.%	wt.%	Atm.%	wt.%	Atm.%	wt.%
RA1		66.26	54.40	12.75	7.86	7.63	11.00	12.25	25.20	1.11	1.54	-	-	-	-
RA2		65.07	54.78	16.32	10.31	5.77	8.53	11.39	24.02	0.74	1.05	0.36	0.61	0.34	0.69
RA3		62.95	54.06	19.38	12.49	6.01	9.06	10.21	21.97	0.77	1.12	0.29	0.51	0.38	0.79

In the first-generation recycled aggregate, from the crushing of a source concrete with natural aggregates only, the presence of sulphur or potassium is not detected. By increasing the volume of adhered mortar, with the second and third generation, the sulphur or potassium increase their concentration and can be detected. In the first generation their percentage is so small that they are not identified by the Energy Dispersive X-ray spectroscopy.

Figs. 9-11-10-12 show a micrograph sequence at 50, 100, 500 and 1000 magnifications of the analysed RA1, RA2 and RA3, respectively. Backscattered electrons micrographs are presented. It is observed that the natural aggregates reduce their size and number with the number of cycles, from RA1 to RA3. The main observed cracks correspond to the ITZ between the new paste and the recycled aggregate. The crack initiation and propagation into the recycled concrete under compression was dependent on the relative strength of the new and old ITZ's [32] Therefore, it is expected that the aggregates recycled more than once lead to progressively less resistant concrete (see Fig. 12).

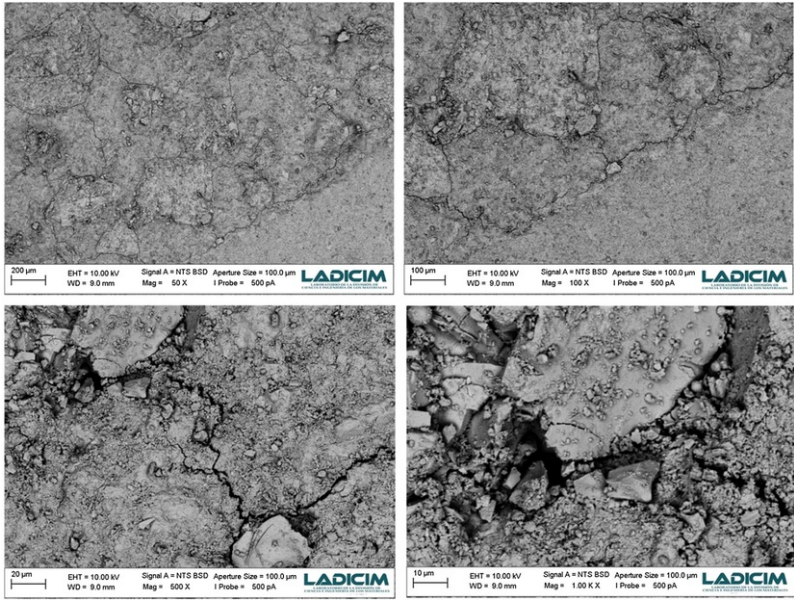


**Fig. 10** Scan electron micrograph sequence (50×, 100×, 500× and 1000×) of a region of aggregate-cement paste interphase of RA1.

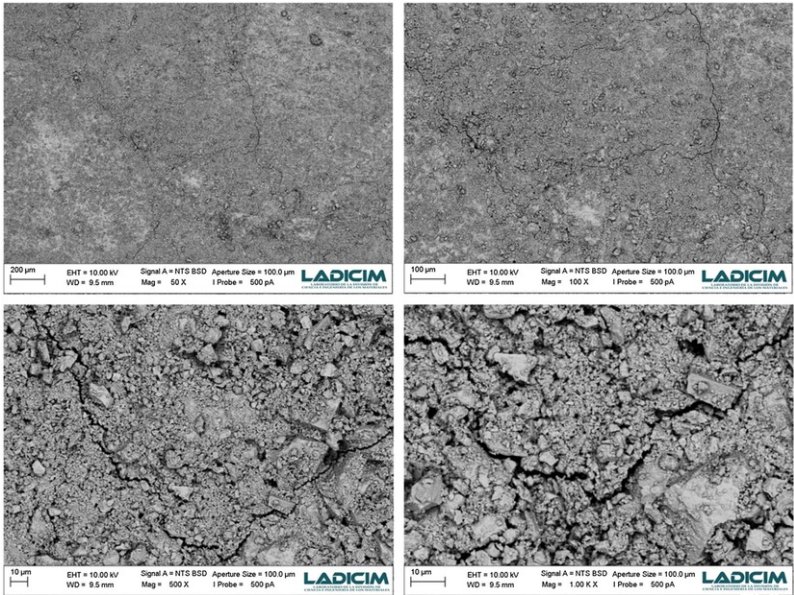


**Fig. 11** Scan electron micrograph sequence (50×, 100×, 500× and 1000×) of a region of aggregate-cement paste interphase of RA2.

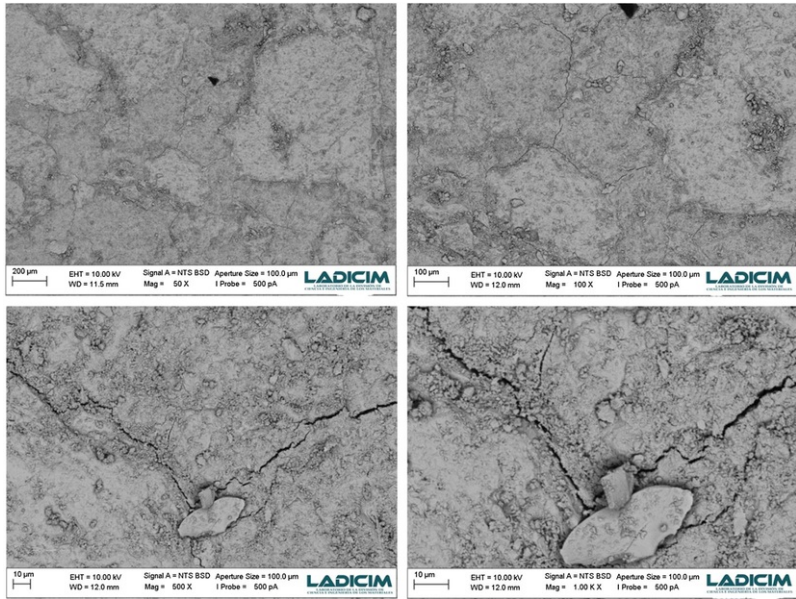


**Fig. 12** Scan electron micrograph sequence (50×, 100×, 500× and 1000×) of a region of aggregate-cement paste interphase of RA3.

With the obtained results by classic and new methods, it is possible to evaluate accurately the volume of adhered mortar of the recycled aggregate. For this purpose, it has been proposed to analyse the properties of concrete with different degrees of recycling, in order to know how it affects the properties of the material and how it could be analysed. In any case, the characteristics of the multi-recycled concrete mixes will depend on the properties of the source concrete, the proposed mix proportions and its cement. A sustainable future implies multi-recycled concrete, so the study of new combinations will be a very important future line of research.

## 4 Conclusions

In the present research, the effect of multiple recycling on the properties of recycled aggregate (from crushed concrete) has been analysed and, in addition, an innovative technique of analysis has been proposed. The following conclusions can be drawn.

- Regarding the physical properties of the aggregate, the first recycling cycle decreases the density and increases the porosity and the absorption significantly more than the second and third recycling cycles. The density of the recycled aggregates decreases as larger aggregates are selected and this effect is the more pronounced the more often the aggregates are recycled.
- The volume taken by the aggregates is greater the more often they are recycled. This effect is due to the higher roundness of their particles and their higher capacity of accommodation. However, the density of the whole decreases and the absorption increases because of the higher volume of adhered mortar.
- Computerized micro-tomography has been shown to be a technique capable to identify the different phases of the recycled aggregate, thus determining the volume of adhered mortar. Microtomography also has shown that the relationship between the volume of natural aggregate and adhered mortar is asymptotically decreasing. It is observed that from the second cycle on this ratio is below 20%.
- After the third recycling cycle, it is observed that the volume of adhered mortar represents more than 80% of the volume of the aggregate. The trend lines predict that, from the fourth cycle on, the original natural coarse aggregate will become negligible and the recycled aggregate will consist of almost 100% mortar.
- Electron microscopy has confirmed the presence of a greater number of cracks and interfaces in the aggregate, as it is recycled a greater number of times. These results confirm the loss of mechanical properties detected in the Los Angeles coefficient tests.

## 5 Uncited reference

[27].

## Acknowledgments

The authors would like to thank:

LADICIM, Laboratory of Materials Science and Engineering of the University of Cantabria and Instituto Superior Técnico of the University of Lisbon for making available to the authors the facilities used in this research.

The Erasmus+Program, founded by the Staff Mobility for Teaching Program of the European Council 2016/217, between Instituto Superior Técnico - University of Lisbon and the LADICIM - University of Cantabria.

CERIS and the Foundation for Science and Technology (FCT) for funding this research.

## References

- [1]** B. González-Fontebo and F. Martínez-Abella, Shear strength of recycled concrete beams, *Constr. Build. Mater.* **21**, 2007, 887–893.
- [2]** S. Seara-Paz, B. González-Fontebo, F. Martínez-Abella and I. González-Taboada, Time-dependent behaviour of structural concrete made with recycled coarse aggregates. Creep and shrinkage, *Constr. Build. Mater.* **122**, 2016, 95–109.
- [3]** C. Thomas, J. Setién, J.A. Polanco, I. Lombillo and A. Cimentada, Fatigue limit of recycled aggregate concrete, *Constr. Build. Mater.* **52**, 2014, 146–154.
- [4]** M. Bravo, J. De Brito, J. Pontes and L. Evangelista, Mechanical performance of concrete made with aggregates from construction and demolition waste recycling plants, *J. Clean. Prod.* **99**, 2015, 59–74.
- [5]** R.V. Silva, J. De Brito and R.K. Dhir, The influence of the use of recycled aggregates on the compressive strength of concrete: a review, *Eur. J. Environ. Civil Eng.* **19** (7), 2015, 825–849.
- [6]** D. Pedro, J. De Brito and L. Evangelista, Influence of the use of recycled concrete aggregates from different sources on structural concrete, *Constr. Build. Mater.* **71**, 2014, 141–151.
- [7]** C. Thomas, J. Setién and J.A. Polanco, Structural recycled aggregate concrete made with precast wastes, *Constr. Build. Mater.* **114**, 2016, 536–546.
- [8]** D. Soares, J. de Brito, J. Ferreira and J. Pacheco, Use of coarse recycled aggregates from precast concrete rejects: Mechanical and durability performance, *Constr. Build. Mater.* **71** (0), 2014, 263–272.
- [9]** F. López Gayarre, J. Suárez González, R. Blanco Viñuela, C. López-Colina Pérez and M.A. Serrano López, Use of recycled mixed aggregates in floor blocks manufacturing, *J. Clean. Prod.* **167**, 2018, 713–722.
- [10]** Á. Salesa, J.Á. Pérez-Benedicto, L.M. Esteban, R. Vicente-Vas and M. Orna-Carmona, Physico-mechanical properties of multi-recycled self-compacting concrete prepared with precast concrete rejects, *Constr. Build. Mater.* **153**, 2017, 364–373.
- [11]** V. Corinaldesi and G. Moriconi, The role of industrial by-products in self-compacting concrete, *Constr. Build. Mater.* **25** (8), 2011, 3181–3186.
- [12]** C. Thomas, A. Cimentada, J.A. Polanco, J. Setién, D. Méndez and J. Rico, Influence of recycled aggregates containing sulphur on properties of recycled aggregate mortar and concrete, *Compos. B Eng.* **45** (1), 2013, 474–485.
- [13]** C. Medina, M.I. Sánchez de Rojas, C. Thomas, J.A. Polanco and M. Frías, Durability of recycled concrete made with recycled ceramic sanitary ware aggregate Inter-indicator relationships, *Constr. Build. Mater.* **105**, 2016, 480–486.
- [14]** M. Wijayasundara, P. Mendis and R.H. Crawford, Methodology for the integrated assessment on the use of recycled concrete aggregate replacing natural aggregate in structural concrete, *J. Clean. Prod.* **166**, 2017, 321–334.
- [15]** C. Thomas, J. Setién, J.A. Polanco, P. Alaejos and M.S. de Juan, Durability of recycled aggregate concrete, *Constr. Build. Mater.* **40**, 2013, 1054–1065.
- [16]** Valeria Corinaldesi, Structural concrete prepared with coarse recycled concrete aggregate: from investigation to design, *Adv. Civil Eng.* **2012**, 2011, 1–6.



- [17]** D. Pedro, J. de Brito and L. Evangelista, Structural concrete with simultaneous incorporation of fine and coarse recycled concrete aggregates: mechanical, durability and long-term properties, *Constr. Build. Mater.* **154**, 2017, 294-309.
- [18]** I.F. Sáez del Bosque, W. Zhu, T. Howind, A. Matías, M.I. Sánchez de Rojas and C. Medina, Properties of interfacial transition zones (ITZs) in concrete containing recycled mixed aggregate, *Cem. Concr. Compos.* **81**, 2017, 25-34.
- [19]** H.E. Martz, S.G. Azevedo, J.M. Brase, K.E. Waltjen and D.J. Schneberk, Computed tomography systems and their industrial applications, *Int. J. Radiat. Appl. Instrument.* **41** (10-11), 1990, 943-961.
- [20]** I.L. Morgan, H. Ellinger, R. Klinksiek and J.N. Thomson, Examination of concrete by computerized tomography, *J. Am. Concr. Inst.* **77** (1), 1980, 23-27.
- [21]** M. Zhang, Pore-scale modelling of relative permeability of cementitious materials using X-ray computed microtomography images, *Cem. Concr. Res.* **95**, 2017, 18-29.
- [22]** M.B. Leite and P.J.M. Monteiro, Microstructural analysis of recycled concrete using X-ray microtomography, *Cem. Concr. Res.* **3** (81), 2016, 38-48.
- [23]** C. Thomas, I. Sosa, J. Setién, J.A. Polanco and A.I. Cimentada, Evaluation of the fatigue behaviour of recycled aggregate concrete, *J. Clean. Prod.* **65**, 2014, 397-405.
- [24]** K. Onoue, M. Tokitsu, M. Ohtsu and T.A. Bier, Fatigue characteristics of steel-making slag concrete under compression in submerged condition, *Constr. Build. Mater.* **70** (0), 2014, 231-242.
- [25]** J. Xiao, H. Li and Z. Yang, Fatigue behavior of recycled aggregate concrete under compression and bending cyclic loadings, *Constr. Build. Mater.* **38** (0), 2013, 681-688.
- [26]** C.J. Zega, G.S. Coelho, Y.A. Dos Santos, A.A Di Villagrán-Zaccardi and Maio, Performance of recycled concretes exposed to sulphate soil for 10 years, *Constr. Build. Mater.* **102**, 2016, 714-721.
- [27]** A.M. Braga, J.D. Silvestre and J. de Brito, Compared environmental and economic impact from cradle to gate of concrete with natural and recycled coarse aggregates, *J. Cleaner Prod.* **162**, 2017, 529-543.
- [28]** P. Niewiadomski, D. Stefaniuk and J. Hoła, Microstructural analysis of self-compacting concrete modified with the addition of nanoparticles, *Proc. Eng.* **172**, 2017, 776-783.
- [29]** S. Sunayana and S.V. Barai, Recycled aggregate concrete incorporating fly ash: comparative study on particle packing and conventional method, *Constr. Build. Mater.* **156**, 2017, 376-386.
- [30]** V.W.Y. Tam, C.M. Tam and K.N. Le, Removal of cement mortar remains from recycled aggregate using pre-soaking approaches, *Resour. Conserv. Recycl.* **50** (1), 2007, 82-101.
- [31]** H. Tateyashiki, H. Shima, Y. Matsumoto and Y. Koga, Properties of concrete with high quality recycled aggregate by heat and rubbing method, *Proc. JCI* **23** (2), 2001, 61-66.
- [32]** W. Li, C. Long, V.W.Y. Tam, C. Poon and Duan W. Hui, Effects of nano-particles on failure process and microstructural properties of recycled aggregate concrete, *Constr. Build. Mater.* **142**, 2017, 42-50.

---

## Highlights

- Multiple recycling properties of recycled aggregate has been analysed.
- Computerized micro-tomography identifies phases of the recycled aggregate.
- After 3 recycling the volume of adhered mortar is 80% of the aggregate.
- Density decreases with recycling cycles and the size of the aggregate.

---

## Queries and Answers

**Query:** Your article is registered as a regular item and is being processed for inclusion in a regular issue of the journal. If this is NOT correct and your article belongs to a Special Issue/Collection please contact t.gunasekaran.1@elsevier.com immediately prior to returning your corrections.

**Answer:** Yes

**Query:** The author names have been tagged as given names and surnames (surnames are highlighted in teal color). Please confirm if they have been identified correctly.

**Answer:** They are correct identify but Sainz-Aja was wrong written. Also in the sent manuscript, sorry.

**Query:** Please note that Fig. 12 are not cited in the text. Please check that the citations suggested by the copyeditor are in the appropriate place, and correct if necessary.

**Answer:** There was a mistake at the beginning of the paragraph: Fig. 9-11 was changed by Fig. 10-12.

**Query:** This section comprises references that occur in the reference list but not in the body of the text. Please position each reference in the text or, alternatively, delete it. Any reference not dealt with will be retained in this section.

**Answer:** It was missing at the text. The correct position is the last sentence of the first paragraph of the "2 Experimental program". Please change (27) by [27] I can not write it with [ ].

**Query:** Please check the edit(s) made in Table 5, and correct if necessary.

**Answer:** The table header was corrected.